Hydrothermal liquefaction versus catalytic hydrodeoxygenation of a bioethanol production stillage residue to platform chemicals

Hita, I.; Ghoreishi, S.; Santos, J. I.; Barth, T.; Heeres, H. J.

Published in:
Fuel processing technology

DOI:
10.1016/j.fuproc.2020.106654

Fuel Processing Technology 213 (2021) 106654

Contents lists available at ScienceDirect

Fuel Processing Technology

journal homepage: www.elsevier.com/locate/fuproc

Research article

Hydrothermal liquefaction versus catalytic hydrodeoxygenation of a bioethanol production stillage residue to platform chemicals: A comparative study

I. Hita [a,d,*], S. Ghoreishi [b], J.I. Santos [c], T. Barth [b], H.J. Heeres [a,*]

[a] Chemical Engineering Department, ENTEG, University of Groningen, Nijenborgh 4, 9747, AG, Groningen, the Netherlands
[b] Department of Chemistry, University of Bergen, Allegaten 41, N-5007 Bergen, Norway
[c] Department of Chemical Engineering, University of the Basque Country (UPV/EHU), PO Box 644-48080, Bilbao, Spain
[d] King Abdullah University of Science and Technology, KAUST Catalysis Center (KCC), Multiscale Reactor Engineering, Thuwal 23955-6900, Saudi Arabia

ARTICLE INFO

Keywords:
Bioethanol stillage
Hydrothermal liquefaction
Hydrodeoxygenation
Alkylphenolics
Aromatics

ABSTRACT

Biobased chemicals like phenols and aromatics are preferably produced from cheap biomass waste streams. In this work, we have explored the potential of a eucalyptus-derived second generation bioethanol production stillage (BPS) residue for this purpose. A comparative study between a hydrothermal liquefaction (HTL) and a catalytic hydrodeoxygenation (HDO) step, as well as a 2-step HTL-HDO approach is reported, targeting at value-added low molecular weight platform chemicals (mainly alkylphenols and aromatics). HDO was observed to be a more suitable strategy than HTL for the production of organic oils enriched in valuable monomers. The direct HDO of the BPS using a commercial Ru/C catalyst at 450 °C and 100 bar H_2 pressure led to an organic product oil (30.7 wt%) with a total monomer yield of 25.2 wt% (13.2 wt% of alkylphenolic+aromatics), compared to a 53.2 wt% of a product oil with 10.0 wt% monomers for the HTL step (305 °C). A 2-step HTL-HDO strategy was compared with the direct HDO approach. Comparable alkylphenolic+aromatic yields were obtained through this approach based on initial BPS intake (13.2 wt% vs 12.3 wt% for the direct HDO and HTL-HDO approach, respectively). Lower HTL temperatures (305 °C) for the first step are preferred to prevent over hydrogenation in the subsequent HDO step. As such, HTL appears a suitable pre-treatment for BPS and can (i) solve the issues related to the feeding of solids in pressurized continuous reactors for HDO and (ii) prevent coke formation during the HDO step, thus improving catalyst stability and durability.

1. Introduction

The foreseeable depletion of fossil energy sources combined with strict environmental policies to reduce CO_2 emissions will require the establishment of sustainable and competitive lignocellulose-based (bio) refineries to produce biofuels and biobased chemicals and materials [1,2]. A well-known example is the production of bioethanol as an alternative to traditional fossil-derived gasoline. In this respect, bioethanol derived from non-edible lignocellulosic biomass (second generation bioethanol) is preferred over conventional first-generation bioethanol from sugar sources [3,4]. However, in second-generation processes, significant residual amounts of stillage are produced, and the development of effective valorization routes towards added-value platform chemicals for this material is key in boosting the profitability of the 2nd generation bioethanol industry [5]. A techno-economic analysis by Baral et al. [6] demonstrated higher profitability of using stillage as a source for biobased products instead of using it solely for combustion. However, the material is a complex mixture of lignin, residual (hemi)cellulose, and other residues (e.g. proteins) in variable amounts which renders its conversion highly challenging, and the use of "traditional" routes for technical lignins for this material needs to be explored and understood.

Among the wide variety of lignocellulosic biomass conversion methods available [7], hydrothermal liquefaction (HTL) presents several advantages: (i) no pre-drying is required for the biomass, (ii) hot pressurized water can simultaneously be used as reactant and reaction media, (iii) it requires milder operation conditions in comparison to other approaches (i.e. pyrolysis, gasification) and (iv) is highly versatile

* Corresponding authors at: Chemical Engineering Department, ENTEG, University of Groningen, Nijenborgh 4, 9747, AG, Groningen, the Netherlands.
E-mail addresses: idoia.hitadelolmo@kaust.edu.sa (I. Hita), h.j.heeres@rug.nl (H.J. Heeres).

https://doi.org/10.1016/j.fuproc.2020.106654
Received 20 August 2020; Received in revised form 17 October 2020; Accepted 23 October 2020
Available online 10 November 2020

and environmentally friendly [8,9]. HTL is also applicable to lignin-containing feed streams. So far, most of the lignin liquefaction studies focused either on technical commercially available lignins [10–13] for the production of oils enriched in oxygenated monomers [8] or model compounds, like phenolic dimers. [14] The use of formic acid (which delivers molecular hydrogen when decomposing) in HTL is also known to aid the production of an oil product with increased H/C ratios and lower oxygen contents [15,16].

To date, research reported in the literature on bioethanol production stillage (BPS) residues for the production of platform chemicals is scarce. A BPS from the enzymatic hydrolysis of eucalyptus was recently used by Løhre et al. [17] to obtain monomers through a lignin-to-liquid solvolysis approach in a batch reactor and using FA as a hydrogen donor. They attained oil yields between 26.4 and 36.6 wt%. Besides, it was reported that removal of the carbohydrate fraction in the stillage by an organosolv extraction leads to enhanced oil yields. Liu et al. [18] evaluated the use of corn stalk lignin residues from bioethanol production for the synthesis of a wide range of vinyl phenolics through pyrolysis. Mainly 4-vinylphenol and 4-vinylguaiacol were formed with a selectivity of up to 43.9 wt% at 500 °C. Ru-based catalysts supported over ZrO_2 and activated carbon were applied by Gómez-Monedero et al. [19] on the solvent-aided hydrotreatment of an industrial BPS in a batch reactor resulting in liquid product yields in the 60–70% range. The hydrotreatment of pyrolysis liquids derived from BPS residues was also recently reported by Priharto et al. [20] for the production of monomers, achieving total monomer yields of up to 50 wt%, primarily in the form of alkylphenols. Other advanced bioethanol stillage applications include the use of thermoset biocomposites [21] and the production of adhesives [22], among others.

Despite the potential of HTL for depolymerization of polymeric lignin-containing materials to product oils enriched in phenolics, further upgrading is required to reduce the bound oxygen content and to reduce the molecular weight of the obtained liquefaction oils [9]. In this context, catalytic hydrodeoxygenation (HDO) over noble metal-based catalysts is considered as one of the most promising routes. It involves contacting the biomass-derived feed with a catalyst in combination with hydrogen or a compound that forms hydrogen in situ (e.g. alcohols, formic acid). Examples of catalysts are sulfided NiMo and CoMo catalyst formulations and noble metals on supports, of which the latter have shown to be more active and present higher stability in a water-containing reaction medium [23–26].

In this work, we have assessed the potential of a bioethanol production stillage (BPS) residue, obtained from a mild acid pretreatment followed by enzymatic hydrolysis of eucalyptus, as a source for sustainable biobased platform chemicals (primarily alkylphenols and aromatics). A comparative study has been performed between the direct one-pot HTL and the catalytic HDO (using Ru/C and Pt/C catalysts) and a 2-step HTL-HDO approach, in terms of product yields and the quality and composition of the produced oils at different operation temperatures. The experimental conditions were selected based on available literature on HTL-HDO. HTL is typically conducted at temperatures in the 270–370 °C range [7–9]. In this case, two temperatures (305 °C and 350 °C) were selected to obtain HTL oils with distinct characteristics in terms of polymerization and functionalization degree, oxygen content, and monomer content. Experimental conditions for the HDO reaction (100 bar initial H_2 pressure, 375–450 °C) are in line with those for the HDO of typical lignocellulosic biomass and technical lignins [20,23–26].

Such a comparison between an HTL and HDO approach in general and BPS, in particular, to aim for monomeric aromatic bulk chemicals has not been reported in the literature. Also, a two-step approach (HTL-HDO) was proposed and tested and this is an absolute novelty of this paper. We will show that this approach has advantages compared to the individual steps. Finally, we have not only carefully considered typical engineering aspects of the process like mass- and energy balances, but also assessed in detail the composition of the liquid phases using (advanced) analytical techniques (EA, GCxGC-FID, GPC, ^{13}C NMR), which provided also insights into the molecular transformations occurring during the HTL and HDO processes.

2. Experimental section

2.1. Chemicals and catalysts

The bioethanol production stillage (BPS) residue, produced by a mild acid pretreatment followed by enzymatic hydrolysis of eucalyptus was produced at the Biorefinery Demo Plant (BDP) in Örnsköldsvik (Sweden) and provided by SEKAB (Sweden). The BPS was received as a wet sample and was dried in an oven at 60 °C until constant weight before subsequent manual grinding and sieving to a dry powder ($d_p < 500$ μm). For HDO experiments, the sample was ball milled using a Fritsch GmbH Pulverisette 6 ball miller, for 5 min at 300 rpm. Tetrahydrofuran (> 99.9%), ethyl acetate (> 99.8%), and formic acid (> 98%) were purchased from Sigma Aldrich and used without further purification in the hydrothermal liquefaction (HTL) stage.

The Ru/C and Pd/C catalyst (5 wt% metal loading) used for the catalytic hydrodeoxygenation (HDO) were supplied by Sigma-Aldrich, and their main physicochemical properties have been summarized in Table S1. The surface area, pore-volume, and pore distribution were analyzed using N_2 physisorption at −196 °C in a Micromeritics 2020 setup after a previous 8 h degas at 120 °C under vacuum conditions. Total acidity was measured through NH_3-TPD (temperature-programmed desorption) experiments in a quartz microreactor. The samples were reduced under H_2 at 500 °C for 30 min and subsequently saturated at 150 °C under a 5 wt% NH_3/He mixture. Lastly, TPD measurements were performed up to 600 °C at a 10 °C min^{-1} rate under He and the evolved NH_3 was detected through a thermal conductivity detector (TCD).

Dichloromethane (DCM) and acetone (both purchased from Boom B·V.) were used as solvents for product retrieval in the HDO process. Hydrogen (> 99.99%, purchased at Hoek Loos) was used as the reaction gas. The reference gas used for identification of the permanent gases in the gaseous product was supplied by Westfalen Gassen Nederland B.V (55.19% H_2, 19.70% CH_4, 3.00% CO, 18.10% CO_2, 0.51% ethylene, 1.49% ethane, 0.51% propylene, and 1.50% propane). He (Linde, > 99.99%) was used as the carrier gas for gas product analysis.

For the GCxGC-FID analysis, tetrahydrofuran (THF, Boom B.V.) was used as a solvent, and di-n-butyl ether (DBE, 99.3%, Sigma Aldrich) was used as an internal standard.

2.2. Bioethanol production stillage (BPS) characterization

Elemental analyses (EA) to determine the C, H, N, and S content of the BPS and liquid organic samples were performed using a Euro Vector 3400 CHN-S analyzer. The amount of oxygen was calculated by the difference. Analyses were performed at least in duplicate and average values are reported.

Thermogravimetric analysis (TGA) of the BPS was carried out using a Thermogravimetric Analyzed TGA 4000 apparatus from Perkin-Elmer. Approximately 10 mg of sample was used for each analysis. The sample was heated from 30 to 900 °C at a 10 °C min^{-1} rate under an inert N_2 atmosphere (50 mL min^{-1}). To estimate the cellulose, hemicellulose, and lignin contents in DGS, Gaussian deconvolution was conducted on the DTG curves using Origin 9.0 software by OriginLab.

Proximate analysis of BPS was obtained from experiments in the aforementioned TGA setup. It involves (i) sample stabilization at 35 °C for 5 min under an N_2 atmosphere (50 mL min^{-1}), (ii) heating the sample up to 110 °C at a 40 °C min^{-1} rate, (iii) keeping a 5 min isotherm, (iv) heating up to 950 °C at a 40 °C min^{-1} rate, (v) keeping an isotherm for 5 min, (vi) switching gas to air (50 mL min^{-1}) and (vii) keeping an isotherm for 10 min.

Fourier Transformed Infrared spectra (FTIR, 64 scans) were acquired

using a Spectrum 2000 apparatus from Perkin Elmer. Spectra were obtained in absorbance mode in the 600–4000 cm^{-1} scan range using Happ-Genzel apodization.

^{13}C CPMAS NMR spectra were recorded on a Bruker AVANCE III, 9.4 T system equipped with a 4 mm MAS DVT Double Resonance HX MAS probe. Larmor frequencies were 400.17 MHz and 100.63 MHz for ^{1}H and ^{13}C nuclei, respectively. The sample rotation frequency was 10 kHz and the relaxation delay was 5 s. The number of scans was 10,240. Polarization transfer was achieved with RAMP cross-polarization (ramp on the proton channel) with a contact time of 5 ms. High-power SPINAL 64 heteronuclear proton decoupling was applied during acquisition. The estimated concentration (%) of methoxy functionalities in the BPS was calculated from the integration of the solid-state CP/MAS ^{13}C NMR spectra using Eq. (1).

$$[MeO](\%) = \frac{A_{MeO}}{A_{Total}} 100 \quad (1)$$

Where A_{MeO} is the area of the methoxy peak in the spectra (δ 50–59 ppm) and A_{Total} is the total peak area (δ 0–210 ppm).

2.3. Hydrothermal liquefaction (HTL) of BPS

Hydrothermal liquefaction experiments were carried out in a stirred 5.3 L high-pressure autoclave reactor from ESTANIT GmbH at two different experimental conditions: (i) 305 °C, a reaction time of 2 h; reactor intake: 200 g of BPS, 500 g of water, and 244 g of formic acid (FA) and (ii) 350 °C, a reaction time of 2 h; reactor intake: 300 g of BPS, 750 g of water, and 366 g of FA. The heating time from room temperature to the desired temperature (305 and 350 °C) was in a range of 60–70 min, giving an approximate heating rate of 5 °C min^{-1}. Reaction time was measured after the setpoint temperature was reached. The experiments (and the produced liquefied oils) were designated as HTL1 (305 °C) and HTL2 (350 °C). The workup procedure for the recovery of the different product fractions is given in detail in Scheme S1. The final oil and solid yields were determined by weight after solvent evaporation and drying. The mass balance was calculated as the sum of oil and char yields (Eq. (2).

$$Product\ yield\ (wt\%) = \frac{Dry\ product\ weight\ (g)}{Dry\ BPS\ intake\ (g)} \times 100 \quad (2)$$

2.4. Catalytic hydrotreatment of the BPS and HTL oils

The catalytic hydrotreatment runs were carried out in a stainless steel batch autoclave (100 mL, Parr Instruments Co.) equipped with a Rushton-type turbine as described in previous research [27,28]. During the experiments, temperature and pressure in the reactor were monitored online. For all experiments, the reactor was loaded with 15 g of either ball-milled BPS (direct HDO) or HTL oil (HTL + HDO approach) and 0.75 g of catalyst (Ru/C or Pd/C). After loading the reactor, it was flushed several times with H_2 to expel air and then pressurized to 180 bar for a leak test at room temperature. Subsequently, the H_2 pressure was set at 100 bar, and stirring was started at 1200 rpm. After that, the reactor was heated up to the desired reaction temperature (375–450 °C) at an approximate rate of 10 °C min^{-1}, and time zero was set once the temperature setpoint was reached. After 4 h, the reactor was cooled to room temperature and the pressure at room temperature was recorded. In combination with a compositional analysis of the gas phase by GC, it allowed determination of the total amount of H_2 consumed during the reaction.

The workup protocol followed for the recovery of the different product fractions involves a solvent-based procedure which is described in detail in previous works [29,30] and schematized in Scheme S2. Gas-phase products were collected in a 3 L Tedlar gas bag to determine their composition. After the reaction, an aqueous phase and an organic phase were obtained. The organic oil and water were easily separated from the rest of the products by decantation. After that, a solvent wash was used to recover the remaining organic products absorbed on the solid phase. The procedure involves treatment of the solid phase with DCM and acetone, from where organic DCM and acetone soluble phases are obtained, respectively. The remaining solid fraction, containing both the spent catalyst and the coke formed during the reaction was dried and weighted for mass balance calculations. Product yields and mass balances are calculated on feed intake (either BPS or HTL oils) basis, as specified in Eqs. (3) and (4).

$$Product\ yield\ (wt\%) = \frac{Product\ weight\ (g)}{Feed\ weight\ (g)} \times 100 \quad (3)$$

$$Mass\ balance\ (wt\%) = \frac{\sum(Product\ weight)(g)}{Feed\ weight\ (g)} \times 100 \quad (4)$$

2.5. Analysis of the gas and organic liquid phases

The composition of the gas phase was analyzed by gas chromatography using a Hewlett Packard 5890 Series II GC apparatus equipped with a thermal conductivity detector (TCD), using a Poraplot Q Al_2O_3/Na_2SO_4 column and a molecular sieve column (5 Å) connected in series. The reference gas had the following composition: 55.19% H_2, 19.70% CH_4, 3.00% CO, 18.10% CO_2, 0.51% ethylene, 1.49% ethane, 0.51% propylene and 1.50% propane.

Two-dimensional gas chromatography analyses were performed on the organic liquid product samples using a Trace GCxGC Interscience equipment provided with a flame ionization detector (GCxGC-FID), a cryogenic trap system, and two columns: an RTX-1701 capillary column (30 m × 0.25 mm i.d. and 0.25 μm film thickness) connected to a Rxi-5Sil MS column (120 cm × 0.15 mm i.d. and 0.15 μm film thickness). He was the carrier gas, and a dual jet modulator was used to trap the samples using CO_2 with a modulation time of 6 s. The injector temperature and FID temperature were set at 280 °C. The oven temperature was kept at 60 °C for 5 min and then heated to 250 °C with a rate of 3 °C min^{-1}. The pressure was set at 0.7 bar. Details on the calibration of the GCxGC-FID and relative response factors (RRFs) are given in previous publications [27,30]. The fraction of volatile compounds in the product oil was calculated using Eq. (5).

$$Volatiles\ (\%) = \frac{Total\ monomer\ yield\ (wt\%)}{Organic\ product\ yield\ (wt\%)} \times 100 \quad (5)$$

For the identification of individual components in the HDO oils, GC analyses were performed using a Hewlett Packard 5890 GC provided with an FID detector, coupled with a Quadruple Hewlett Packard 6890 MSD (GC–MS-FID). An RTX-1701 (60 m × 0.25 mm i.d. and 0.25 μm film thickness) GC column was used.

For both GCxGC-FID and GC–MS-FID analyses, the samples were diluted to a 1:30 ratio in THF and then DBE was added to serve as an internal standard. The identification of the main GCxGC components (aromatics, alkylphenols, ketones, acyclic and cyclic alkanes, naphthenes, guaiacols, and catechols) was done by spiking with representative model compounds of the respective component groups and GC–MS-FID analysis.

The molecular weight distributions of the HTL oils, HDO oils, DCM, and acetone soluble liquid fractions, were determined using gel permeation chromatography (GPC) analyses using an HP1100 unit equipped with three 300 × 7.5 mm PLgel 3 μm MIXED-E columns in series in combination with a GBC LC 1240 RI detector. THF was used as eluent (1 mL min^{-1}), toluene was added as a flow marker, and polystyrene standards with different molecular weights were used for calibration of the molecular weight.

Elemental analyses for the oil products were performed to determine the C, H, N, and S content using a Euro Vector 3400 CHN-S analyzer. The amount of oxygen was calculated by the difference of CHNS. Analyses were performed at least in duplicate and average values are reported.

^{13}C NMR measurements of the liquid HTL and HDO oil samples were carried out using a Bruker AVANCE III 600 MHz spectrometer. Spectra were acquired at 25 °C using an inverse-gated decoupling sequence to avoid the NOE effect, acquiring 2018 scans and using a relaxation delay of 5 s. Dimethyl sulfoxide-d_6 (DMSO-d_6, 99.5 atom%, Sigma Aldrich) was used as a solvent, and deuterated chloroform (99.8 atom%, Sigma Aldrich) was used as an internal standard (IS). The concentration of the samples was 20–22 wt% (approximately 0.2 g of oil in 1 g of solvent), and 0.1 g of IS was added to each sample.

2.6. Energy balances and hydrogen consumption

The energy efficiency of the valorization strategies proposed in the manuscript (HTL of BPS, HDO of BPS, and 2-stage HTL-HDO approach) was calculated using Eq. (6).

$$\eta = \frac{y_{OP}.HHV_{OP}}{HHV_{Feed} + y_{H2}.HHV_{H2}}.100\% \quad (6)$$

Here y_{OP} is the yield of the organic liquid from the HDO of either BPS or an HTL oil, HHV_{OP} is the high heating value of the organic products, HHV_{Feed} is the high heating value of the feed for the HDO process (either BPS or an HTL oil), y_{H2} is the hydrogen consumption per g of feed and HHV_{H2} is the high heating value of hydrogen, which is taken as 141.8 MJ kg^{-1}. HHV_{OP} and HHV_{Feed} were calculated based on the elemental composition (on a dry basis) of the feed and products using Milne's equation and considering the ash content [31]. The y_{H2} was calculated using Eq. (7), assuming ideal gas behavior.

$$yH_2 = \frac{\frac{(P_1 - P_2)\ V_{reactor}\ Mw_{H2}}{R\ T}}{m_{Feed}} \text{ (g/g feed)} \quad (7)$$

Here P_1 and P_2 are the initial and final reaction pressure in the batch reactor at room temperature, $V_{reactor}$ is the reactor volume, Mw_{H2} is the molecular weight of hydrogen, R is the ideal gas constant, T is room temperature (298 K), and m_{Feed} is the initial feed intake.

3. Results and discussion

3.1. Characterization of the BPS

Detailed characterization of the BPS was performed to determine its composition and to gain insights into chemical transformations during HTL and HDO. The elemental composition, proximate analysis, and metal content of the BPS (as calculated from elemental analysis, TG analysis, and ICP) are displayed in Table 1. While the H (5.2 wt%) and N (< 1 wt%) contents are similar to those of commercial (technical) lignins, the C (47.9 wt%) and O (46.3 wt%) contents differ notably (62–68 wt% C and 26–31 wt% O) [28]. The high oxygen content is attributed to a significant amount of residual sugars/carbohydrates present in the BPS material (vide infra) [32]. The nitrogen content (0.6 wt%) also indicates the presence of some residual proteins [33], whose content is estimated to be about 3.8 wt% when using a well-established nitrogen-to-protein conversion factor of 6.25 [34]. Through proximate analysis, a 1.5 wt% moisture content was measured, as well as a 74.4 wt% volatile matter and a 19.1 wt% fixed carbon. The ash content is about 5 wt%, which is in line with data from Løhre et al. [17]. The Klason lignin content was shown to be 51.3 wt%, hence indicating the presence of a significant fraction of acid-insoluble recalcitrant lignin.

TGA analysis was applied to study the thermal behavior of the BPS [28,35]. The TGA and DTG curves (obtained in an N_2 atmosphere) are displayed in Fig. 1. The residue after the measurement was 16%, in contrast to the 30–40 wt% weight residue that is typically observed for commercial (technical) lignins [28,36]. This implies that DGS contains less lignin and more holocellulose, in line with the Klason lignin content analysis [37,38]. The decomposition of the BPS takes place in a wide temperature range and peaks for hemicellulose decomposition at

Table 1
Elemental composition, proximate analysis, and metallic content of the BPS.

Composition	wt%
C	47.9
O	46.3
H	5.2
N	0.6
S	< 0.01

Proximate analysis	wt%
Moisture	1.5
Volatile matter	74.4
Fixed carbon	19.1
Ash	5.0

Other elements	mg kg^{-1}
Al	1034
Ca	9343
Fe	1120
K	723
Mg	439
Na	2008
P	1620

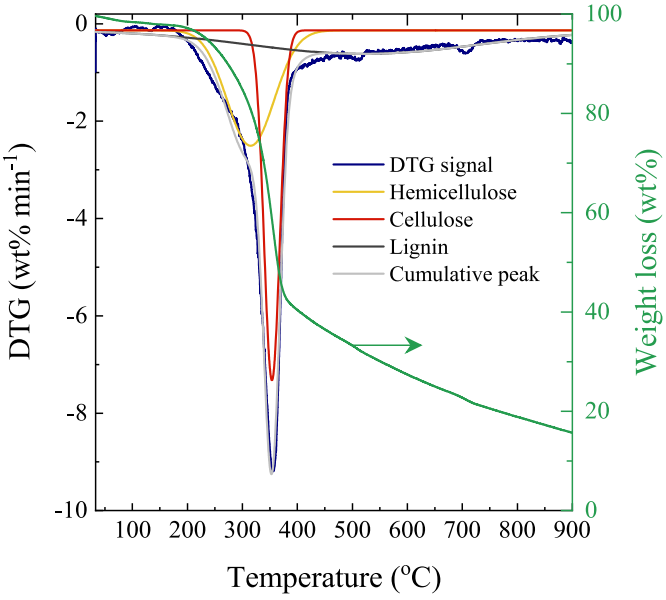

Fig. 1. TGA and DTG curve deconvolution for the thermal BPS decomposition.

200–300 °C, cellulose at 315–400 °C, and lignin at 280–500 °C are observed [39,40]. Through deconvolution of the DTG signal (see Fig. 1) it was estimated that BPS contains 31 wt% of hemicellulose, 36 wt% of cellulose, and 33 wt% of lignin.

Solid-state CP/MAS ^{13}C NMR for the BPS material (Fig. 2) shows intense peaks from the aforementioned residual (hemi)cellulose fraction at δ 64 (C_5), 75 (C_2-C_4), and δ 102 ppm (C_1). Furthermore, characteristic bands for lignin are also observed at δ 50–59 ppm (indicative of the presence of methoxy functionalities), and in the δ 110–160 ppm and δ 165–180 ppm ranges, attributed to C—C double bonds in olefins/aromatics and C═O bonds in lignin, respectively [41,42]. The most intense band in the aromatic region corresponds to aromatics with -OH/-OR substituents. The estimated methoxy content in the BPS (Eq. (1)) is 5.2%, which is about half of the number of methoxy groups typically found in technical lignins [28]. This again confirms that the BPS contains considerable amounts of residual sugars, in agreement with the

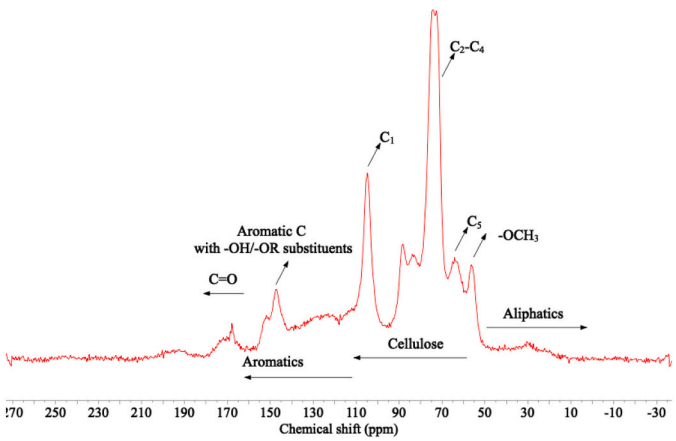

Fig. 2. Solid-state CP/MAS ^{13}C NMR spectra of the BPS.

elemental analysis and TG analysis results in Table 1 and Fig. 1, as well as the FTIR results in Fig. S1, and the Klason lignin analysis.

3.2. Direct hydrodeoxygenation (HDO) of the BPS

The hydrotreatment of BPS was carried out at 375–410-450 °C (Ru/C) and 410–450 °C (Pd/C) using 100 bar hydrogen pressure in a batch set-up in the absence of an external solvent. Typically, a solid phase, two liquid phases (water and organics), and a gas phase were obtained after the reaction. The product distributions are displayed in Fig. 3. An organic liquid phase (oil) was the main product in all cases with yields of 28.0–39.2 wt% on BPS intake, followed by gas products (20.8–23.8 wt %), an aqueous phase (15.1–20.3 wt%), and char (13.5–17.6 wt%). Mass balances were overall satisfactory and > 84% in all cases. Most accurate mass balance closures were achieved at lower hydrotreatment temperatures. This is due to a lower extent of gasification occurring at these temperatures, which is most difficult to quantify accurately. Reproducibility tests showed <3 wt% deviation in the produced yields, indicating good reproducibility and comparability of results.

Analyses of the gas phase products (see detailed composition in Table S2) show the presence of considerable amounts of CO_2 (23.5–25.9%) and CH_4 (10.0–30.0%) and unreacted excess hydrogen. CH_4 is most likely formed from the hydrogenolysis of methoxy functional groups and gas-phase reactions of CO and CO_2 with hydrogen [43]. The formation of CH_4 was significantly higher with the Ru-based catalysts than with the Pd-based one. This is in line with the literature data, showing that Ru is a better methanation catalyst [29].

Typically, the product oils were obtained as viscous oils that required a solvent-based procedure for their isolation (see Scheme S2), particularly when obtained at 375 °C and 410 °C. However, at 450 °C the organic product oil was a clear low-viscous liquid, which could easily be separated from the water phase. Overall, the best results were obtained using the Ru/C catalyst at 450 °C, producing an oil yield of 30.7 wt% and the highest total monomer yield of 25.2 wt%. When operating at the same temperature, the Pd/C catalyst provided higher oil yields compared to the Ru/C catalyst, but less total monomers. This can be explained by assuming a lower cracking activity for the Pd/C catalyst. This eventually leads to a higher amount of higher molecular weight compounds in the product oil compared to the Ru/C catalyst.

The elemental composition (data as obtained) of the product oils is provided in Table S3, and the corresponding O/C and H/C ratios are plotted in the Van Krevelen graph in Fig. 4. Through the direct HDO of the BPS, the oxygen content has been drastically reduced from 46.3% in the BPS (O/C ratio of 0.73) to ca. 3.9–6.3% in the organic product oils (O/C ratio of 0.04–0.06). A slight reduction of the H/C ratio in the oils was also observed compared to BPS. Interestingly, at higher temperatures (450 °C), hydrogenation is promoted and higher H/C ratios are observed in the produced oils (H/C = 1.3). On the other hand, the O/C and H/C ratios are not significantly different for the catalyst. It should also be mentioned that there is always a "residual" amount of oxygen remaining in the organic product (5–7%), and quantitative "deep" deoxygenation towards hydrocarbons is not possible at these conditions.

The composition of the organic product was analyzed using GCxGC-FID, which is known to offer great potential for analyzing highly complex mixtures since components of similar chemical nature can be clustered in specific regions [27,29,44]. An example of a typical chromatogram of bio-derived oils is provided in Fig. S2, where the chemical compounds are classified as alkylphenols, aromatics, naphthalenes, linear and cyclic alkanes, guaiacols, catechols, and ketones [30]. Fig. 5 shows the results obtained using this technique. The total monomer yield from the direct HDO oils (measured by GCxGC-FID), also indicated in Fig. 3 (striped areas), is between 10.8 and 25.2 wt% on BPS intake. It was observed that, even though lower hydrotreatment temperatures favor oil yields (Fig. 3), theamount of monomers is lowest. For instance, in the 375–410 °C range, the organic product volatility (Eq. (4)) was 28–41% (relative to the total), and this value increased up to 65.3% and 82.0% using the Pd/C and Ru/C catalysts, respectively when operating

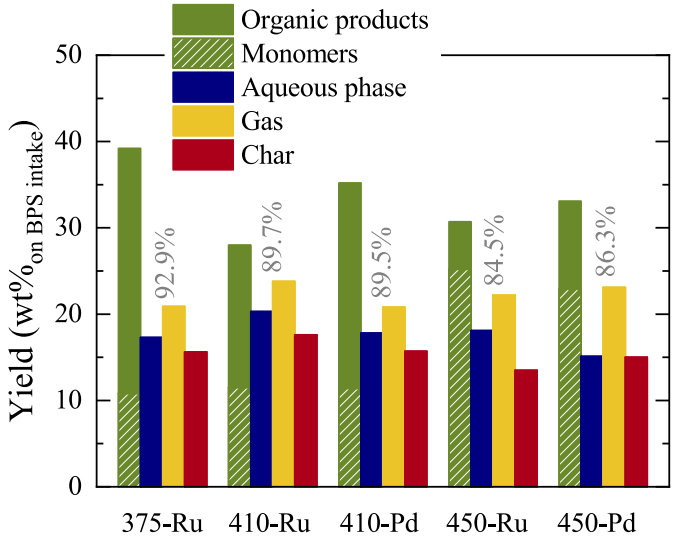

Fig. 3. Main product distribution, total monomer yield, and mass balance closures for the direct hydrotreatment of the BPS with the different catalysts and reaction temperatures.

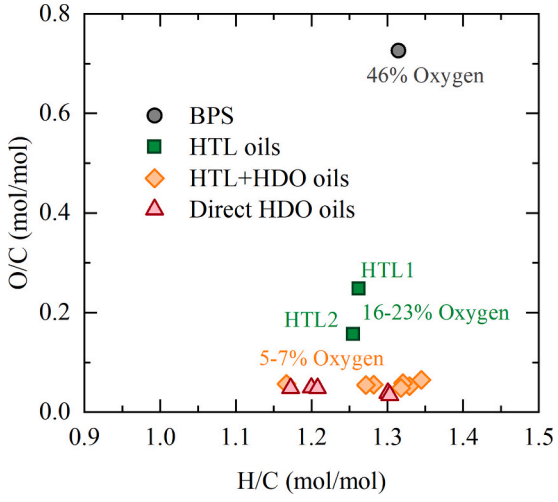

Fig. 4. Van Krevelen plot of the BPS material, the HTL oils, and the oils upgraded through the HDO and HTL-HDO strategies.

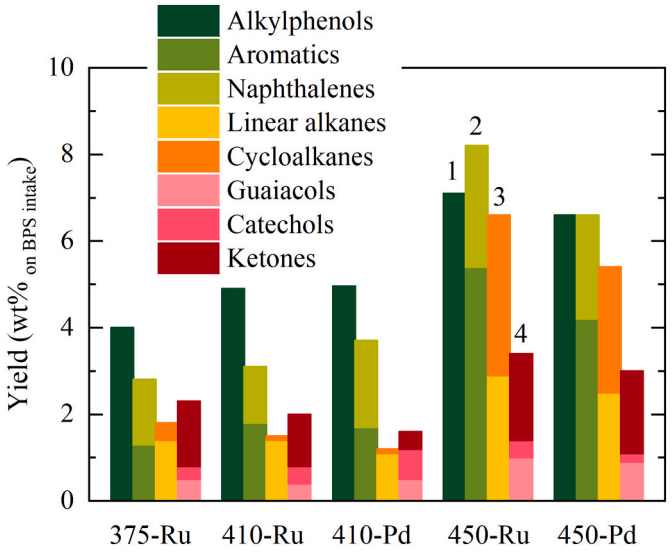

Fig. 5. Organic product composition obtained from the direct hydrotreatment of the BPS classified as: alkylphenols (1), aromatics (2), alkanes (3), and other oxygenates (4).

at 450 °C. Thus, the temperature has a major effect on the level of depolymerization of the BPS, with higher temperatures leading to a higher extent of depolymerization, favoring monomer formation.

Overall, alkylphenols were the main chemical group, together with noticeable amounts of aromatic compounds and (typically) lower amounts of alkanes and other oxygenates. The product composition is temperature depending. In the 375–410 °C range, the amount of both linear and cyclic alkanes is low (< 2 wt%), at higher temperatures (450 °C) their amounts are significantly higher (5.4–6.6 wt%). At 450 °C both linear and cyclic alkanes appear in similar proportions, however, at lower temperatures linear alkanes are dominant. These results can be explained by assuming that both (hydro-) cracking and hydrogenation reactions are enhanced at more severe conditions. As such phenolics and aromatics may be further hydro(deoxy)genated leading to the formation of saturated rings [29,45]. A simplified overview of the lignin fraction related reactions that occur during the HDO of the BPS is provided in Fig. 6. Firstly, the BPS will decompose into smaller mono- and poly-oxygenated compounds through a series of ring-opening, chain scission, cracking and hydrogenation reactions, among others. Subsequently, and even though some of these structures might again condense towards coke, they can undergo either hydrogenation (towards over hydrogenated oxygenated compounds) or hydrodeoxygenation, leading to interesting monomers like monoaromatics, which might also further hydrogenate.

The large influence of reaction temperature on the monomer yields for the different HDO oils was confirmed by their molecular weight distributions as determined by GPC (Fig. S3). The average molecular weights varied from 430 g mol^{-1} at 375 °C, to 290–310 and 220–240 g mol^{-1} at 410 °C and 450 °C, respectively. The GPC curves also show slightly wider distributions (longer tailing) for the oils produced with the Pd catalyst, which is in agreement with their lower volatility when compared to the oils produced using the Ru catalysts (32 vs 41% at 410 °C and 69 vs 82% at 450 °C).

3.3. Hydrothermal liquefaction (HTL) of BPS

The hydrothermal liquefaction of the BPS was carried out in a batch reactor set-up at two different temperatures (305 °C and 350 °C), for 2 h, using water as the solvent and formic acid (FA) as a hydrogen donor in a BPS /H_2O/FA mass ratio of 1/2.5/1.22. For two experiments conducted in the same experimental setup (0.025 L scale) at similar conditions, variations <5% in the product yields were observed. The experiments and corresponding product oils were designated as HTL1 (305 °C) and HTL2 (350 °C). The product distributions for both experiments, together with the chemical composition of the product oils are listed in Table 2. HTL1 was obtained in a yield of 53.2 wt% on a BPS intake basis, together with 23 wt% of char. The remaining products were gases. Performing

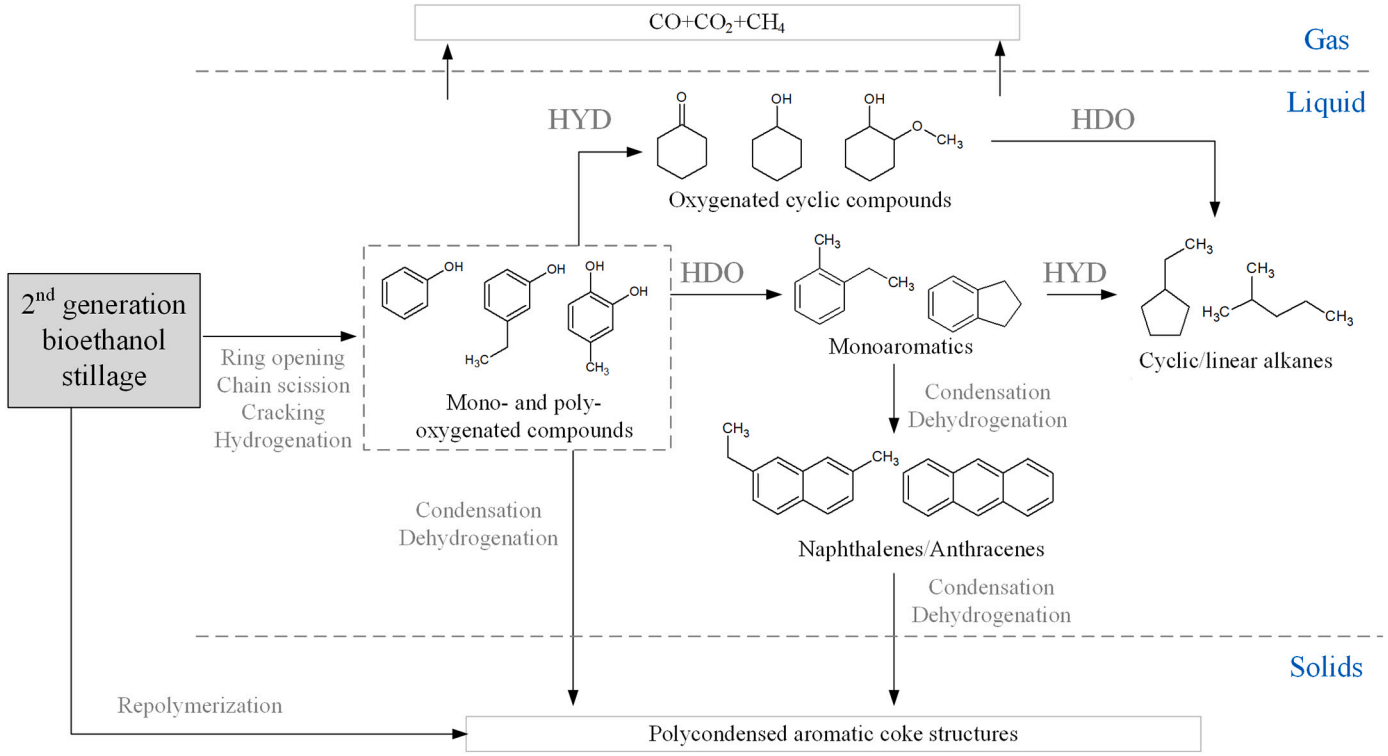

Fig. 6. Simplified scheme of the main lignin-related reactions occurring during the HDO of BPS.

Table 2
Product yields and composition of the oils (as measured from GCxGC-FID) obtained from the hydrothermal liquefaction of the lignin-enriched residue.

	HTL1	HTL2
Oil (wt%)	53.2	43.5
Char (wt%)	22.9	14.7
Material recovery (wt%)	76.1	58.2
Chemical composition of the obtained HTL oils (wt% on BPS intake)		
Alkylphenols	1.9	6.9
Aromatics	0.2	1.1
Naphthalenes	0.3	0.8
Alkanes	0.1	0.5
Cycloalkanes	<0.1	<0.1
Guaiacols	1.3	3.1
Catechols	2.7	8.2
Ketones	1.4	3.2
Fatty acids	0.7	1.1
VFA	1.3	1.7
Volatile fraction (%)	10.0	26.6

the reaction at a higher temperature (HTL2) led to a reduction in oil (43.5 wt%) and char yield (14.7%).

At similar conditions of 310 °C, Duan et al. [46] reported a 60 wt% oil yield from the HTL of alkali lignin in a water/ethanol mixture. In the 300–350 °C range, Rana et al. [47] produced 35.7–38.9 wt% total bio-oil from the depolymerization of Kraft lignin through HTL in subcritical water conditions, accompanied by 27.4–29.1 wt% char formation. All in all, our yield data are consistent with those reported in the literature and prove that the HTL of a BPS can provide comparable oil yields to technical lignins, with less char formation, given the intrinsic lower aromaticity of this material [28].

Through this HTL approach, oils with a partially reduced oxygen content were produced, as shown from the elemental compositions of the HTL oils listed in Table 3 and also in the Van Krevelen plot in Fig. 4. The O/C ratio of the HTL oils was hence decreased to 0.25 (for HTL1) and 0.16 (for HTL2), while the H/C ratio was of 1.2–1.3. Oxygen content has been reduced to 22.9% and 15.8% in the HTL1 and HTL2 oils, implying a total oxygen removal of 50% and 66%, respectively. It should also be mentioned that increasing HTL temperatures favor the removal of oxygen in the product oil [48].

The composition of the volatile fraction of the HTL oils (as measured from GCxGC-FID techniques, following the same chemical group classification discussed in the previous section and including fatty acids and volatile fatty acids, VFA) is provided in Table 2. Oxygenated chemical groups (catechols, ketones, guaiacols, alkylphenols, and fatty acids) accounted for the majority of the volatile fraction of the HTL oils, with total relative concentrations of 93.8 and 90.9% for HTL1 and HTL2, respectively. A higher relative amount of hydrocarbons upon increasing the severity of the HTL process was observed. These results are in line with previous studies on lignin HTL, where lignin is reported to provide mainly phenolic-type compounds in the product oils in comparison to biomass itself [13,49]. Despite significant lignin depolymerization taking place during HTL, the overall volatility of the produced oils was low. The temperature has a major effect and higher process temperature led to higher volatilities, from 10.0% in HTL1 to 26.6% in HTL2, though it is clear that the majority of the oils consist of non-GC detectable components. In line with this, Fig. S4 depicts the GPC distributions for both HTL1 and HTL2 oils, from which the estimated average molecular weights of 840 g mol^{-1} and 420 g mol^{-1} were calculated, respectively.

Table 3
Elemental composition and ^{13}C NMR quantification for the HTL oils.

	HTL1	HTL2
Elemental composition (wt%)		
C	69.3	75.6
H	7.3	7.9
O	22.9	15.8
N	0.5	0.7
^{13}C NMR quantification (%)		
Carbonyl	0.3	1.4
Total aromatics	60.3	49.1
C—O[a]	14	18
C—C[a]	41	36
C—H[a]	45	45
Oxygenated aliphatics	0.9	9.5
MeO	0.7	2.1
Aliphatic side chains	37.8	38.0
Aromatics/Aliphatics[b]	1.6	1.0

[a] Referred to the total aromatic content.
[b] Molar ratio, including oxygenated aliphatics and aliphatic side chains.

Due to the low volatility of the HTL oils and thus the limited identification potential provided by GC techniques, ^{13}C NMR was used to obtain further insights into the chemical composition of the HTL oils. The ^{13}C NMR spectra for both HTL oils is provided in Fig. S5, where the following main regions of interest can be distinguished: the aromatic region in the δ 102–155 ppm range where C—H (δ 95.8–132 ppm), C—C (δ 132–142 ppm) and C—O (δ 142–166.5 ppm) bonds appear; oxygenated aliphatics in the δ 60.8–95.8 ppm range with a strong peak corresponding to the presence of methoxy groups at δ 55.2–60.8 ppm; and saturated aliphatic chains in the 0–55 ppm range (excluding the solvent) [50,51]. The peaks corresponding to the DMSO-d_6 solvent and internal standard (chloroform-*d*) appear at δ 79 ppm and δ 40 ppm, respectively. The quantification results in Table 3 show the predominantly aromatic nature (49–60%) of both HTL oils, particularly in the case of HTL1. In the aromatic region, C—H bonds are predominant (45%), followed by C—C bonds (36–41%) and lower amounts of C—O linkages (14–18%). Sidechain aliphatics account for about 38% in both oils. Interestingly, while in the case of the HTL1 oil (with a higher O_2 content) the majority of the oxygen is contained within aromatic structures, the HTL2 oil presents an important amount of oxygenated aliphatic side chains and methoxy functionalities (9.5 and 2.1%, respectively), which can potentially represent a drawback when the production of phenolic monomers is aimed.

Despite a significant oxygen removal being achieved through HTL, the low volatility of the oils and the significant content of methoxylated oxygenates indicate the necessity of further depolymerization of the HTL oils for obtaining aromatic monomers. Hence, the HDO of these oils will be explored, and the results are provided in the next section.

All in all, and compared to HTL, the direct HDO of the BPS (discussed in Section 3.2.) is a more suitable approach if the production of platform chemicals is targeted. Direct HDO of the BPS provides overall lower oil yields but with a significantly higher volatility and richer in aromatics and (alkyl)phenols, especially when performed at temperatures >410 °C, and with a lower char formation in contrast to HTL. Based on the obtained results, HTL could serve as an interesting pre-treatment for the BPS material when aiming for its valorization in a continuous system, avoiding the hurdles of feeding a solid feedstock in the system, and this approach will be discussed in the following section.

3.4. Two-step HTL-HDO

To the feasibility of a two-step HTL-HDO approach, the HTL oils were subjected to a catalytic hydrotreatment in a batch set-up using molecular hydrogen without the use of an external solvent. The HTL1 oil (of a heavier and more oxygenated nature) was hydrotreated at 410–450 °C using both the Ru/C and Pd/C catalysts, while the HTL2 was processed at milder conditions (410 °C with the Pd/C catalyst and 375–410 °C using the Ru/C catalyst). These are typical hydrotreatment conditions based on literature data and our previous experience reported on hydrotreatment of biomass and bio-liquids [28,52,53]. HDO at 450 °C was not considered to avoid over hydrogenation of the produced organic fraction to alkanes. The product distributions for the hydrotreatment of the HTL1 and HTL2 oils are shown in Fig. 7. The most noticeable result using the 2-step HTL + HDO approach in contrast to direct HDO of the

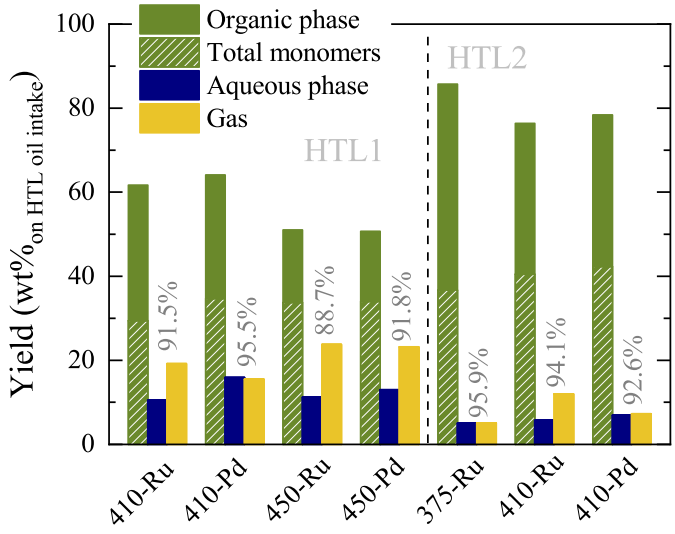

Fig. 7. Main product distribution, total monomer yields, and mass balance closures for the hydrotreatment step in the two-step HTL-HDO approach.

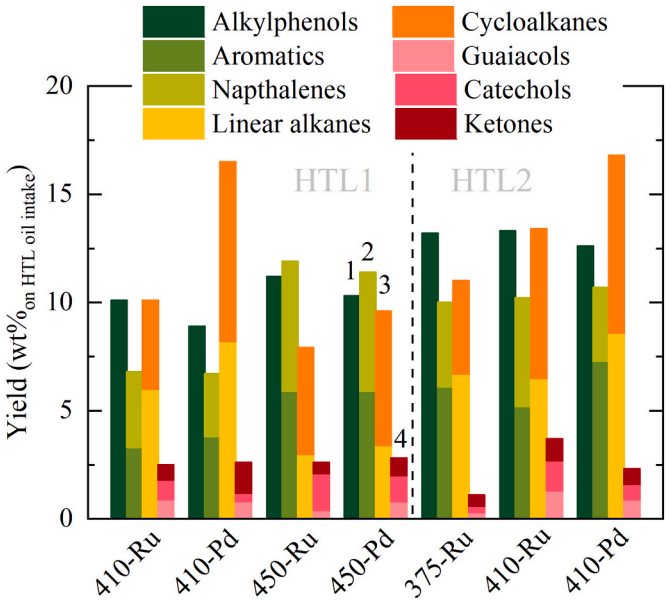

Fig. 8. Organic product composition obtained from the hydrotreatment of the HTL oils classified as alkylphenols (1), aromatics (2), alkanes (3) and other oxygenates (4).

BPS (see Fig. 3), is the absence of char at all temperature conditions and regardless of the catalyst type. Product oil yields were in the 50.7–64.1 wt% (HTL1) and 76.4–85.7 wt% ranges (HTL2). Gas products and aqueous phase yields are higher for HTL1 (15.5–23.8 wt% vs. 5.1–12.0 wt% and 10.5–15.9 wt% vs 5.0–6.9 wt%, respectively). Mass balance closures were between 88.7 and 95.9%. Higher oil yields were obtained at lower temperatures due to a reduction in the number of gas-phase components formed. This observation is in agreement with a study of Shakya et al. [54] on the HDO of an algae bio-oil over different catalysts at 300–350 °C.

The elemental composition for the oils upgraded through the 2-step procedure and those obtained from the direct HDO of the BPS material of these oils are within close ranges (Table S3). As observed from the Van Krevelen plot (Fig. 4) the oils obtained through the HTL-HDO approach show a very similar O/C ratio (0.04–0.06), but an overall higher H/C ratio (1.26–1.35) that those obtained from direct HDO of BPS (1.16–1.22). This is a consequence of processing an already partially deoxygenated and depolymerized feed like the HTL oils, which might lead to over hydrogenated product (see Fig. 6).

Total monomer yields (stripped areas) as determined by GCxGC exceeded 30 wt% in all cases. This is considerably better than for the direct HDO of the BPS, where yields higher than 20 wt% could only be attained at the most severe conditions (450 °C). Furthermore, the molecular weight distributions (see Fig. S4) show that the HTL oils present average molecular weights of 840 g mol^{-1} (HTL1) and 420 g mol^{-1} (HTL2), which have been reduced to 240–270 g mol^{-1} and 210–220 g mol^{-1} when operating at 410 °C and 450 °C, respectively. These results showcase the substantial depolymerization that is occurring during HDO.

The composition of the product oils is displayed in Fig. 8, following the same chemical compound classification applied for the HDO of BPS in Fig. 5. Overall, there is a predominance of alkylphenols and aromatic monomers (combined 12.7–20.0 wt%) in the hydrotreated oils. It is observed that aromatics are preferentially formed at 450 °C when HDO reactions are favored [30]. Alkanes were also observed (23–48 wt%) and among others might originate from the conversion of organic acids in the HTL oils, and over-hydrogenation of aromatics/alkylphenols [54]. The amount is highest when using the Pd/C catalyst, with has a known higher hydrogenation capacity than Ru/C [29], The yields of oxygenated compounds (excluding phenolics) were minor, and in the 2.3–3.6 wt% range. The lower selectivity of the Ru/C catalyst towards the formation of alkanes implies that this catalyst is preferred for the hydrotreatment of the HTL oils. Despite achieving an increase in the product oils of about 15–20 wt% when processing the HTL2 oil at 410 °C (see Fig. 7), monomer yields did not increase proportionally and the oil volatility was in the 43–58% range in all cases at this condition. The highest volatility of 66–67% was attained during HDO at 450 °C.

3.5. *Comparative overview of the direct HDO, HTL, and 2-step HTL-HDO strategies*

In this section, an overview and assessment regarding the energy efficiency, product yields, and compositions obtained from the direct HTL and HDO of BPS and the 2-step HTL-HDO approach are provided. The energy efficiency (Fig. 9) for each route was calculated using the liquid product yields, in combination with the elemental compositions

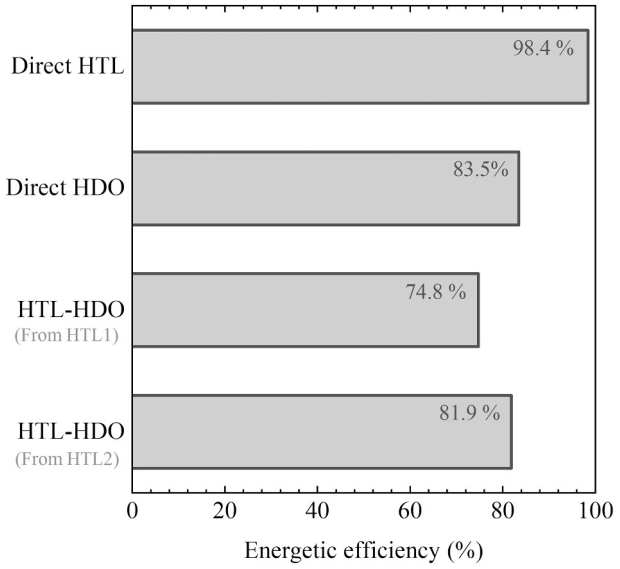

Fig. 9. Energy efficiencies using the best-case experiments for the i) direct conversion of BPS through HTL and HDO, and ii) the 2-step HTL-HDO strategies.

(dry basis) of the BPS feed and the liquid products. The latter was used to calculate the HHV using the Milne equation [31]. The hydrogen consumption was estimated using Eq. (7). An overview of all data is given in Table S4 in the supporting information. The direct HTL of BPS to the HTL oil is very energy efficient, with values of 98.4% for HTL1 oil (HTL at 305 °C) and 92.7% for HTL2 oil (HTL at 350 °C). The best result regarding the direct HDO of BPS was slightly lower and 83.5%, obtained with the Ru/C catalyst at 375 °C. For the two-step process, the energy efficiency was 74.8% using the HTL1 oil as a feed with the Pd/C catalyst at 410 °C, while it was 81.9% for the HTL2 oil using the Ru/C catalyst and at 375 °C. Overall, the highest energy efficiencies have been obtained at the lowest temperatures in the studied ranges as a consequence of lower gas and solid product yields as well as a lower hydrogen consumption. We can also conclude that the energy efficiency for the HTL step is highest. However, as will be discussed later, the amounts of desired monomers are much lower in these oils. For the two-step approach, the efficiency is slightly lower than for the direct HDO.

In the second part of this comparative overview, the focus will be on the monomer yields, and particularly on the yields of the desired alkylphenolics and aromatic compounds. Fig. 10 provides a comparison of the total monomer, alkylphenols, and aromatic yields as obtained for all the conditions reported in this study expressed on an initial BPS weight intake basis.

Our results imply that the one-step HDO approach is better for the production of monomers from BPS than the ones step HTL (sections 3.2 and 3.3, respectively). Performing the direct HDO of BPS at temperatures >450 °C gives oil yields in the range of 30–32 wt% with high volatility, especially when using the Ru/C catalyst (25.2 wt% total monomers). Furthermore, HDO also leads to lower amounts of char formation compared to HTL. All in all, HTL at 305–350 °C provides higher oil yields (43.5–53.2 wt%) than HDO, but of a heavily polymerized nature and with abundant oxygenated functionalities.

When comparing the direct HDO with the 2-step HTL-HDO approach, the most noticeable improvement is the complete absence of coke formation during the HDO stage in the two-step approach, which is likely related to the partially depolymerized nature of the HTL oils.

When assessing the monomer yields (on an initial BPS intake) for the 2-step HTL-HDO approach compared to the one-step HDO, we found that total monomer yields are enhanced from 11.5 to max 18.5 wt% on initial BPS intake when performing the HDO step at 410 °C (Fig. 9a). However, the yields of aromatic and phenol monomers are not proportionally improved for the two step HTL-HDO approach due to over hydrogenation to alkanes. The highest alkylphenol+aromatic yield for the two-step approach was 10.3 wt% on BPS intake (from the HDO of the HTL2 oil at 410 °C) and 12.3 wt% on BPS intake (from the HDO of the HTL1 oil at 450 °C).

The results imply that a two step strategy may be very convenient for future scale-up in continuous pressurized systems. Here, HTL serves as an excellent pre-treatment for BPS providing a liquid that overcomes feeding issues when feeding a solid in a continuous pressurized reactor. A plausible strategy could be to conduct a preliminary low/mild temperature HTL (obtaining a viscous liquid rich in oxygen) and a subsequent high-temperature HDO, where char formation is minimized and hence catalyst lifetime is prolonged and stability is improved (no clogging). To avoid the observed over hydrogenation of the desired alkylphenols/aromatics to alkanes, the use of catalysts with lower metal content and/or the use a less active metal, like Ni or Mo need to be explored.

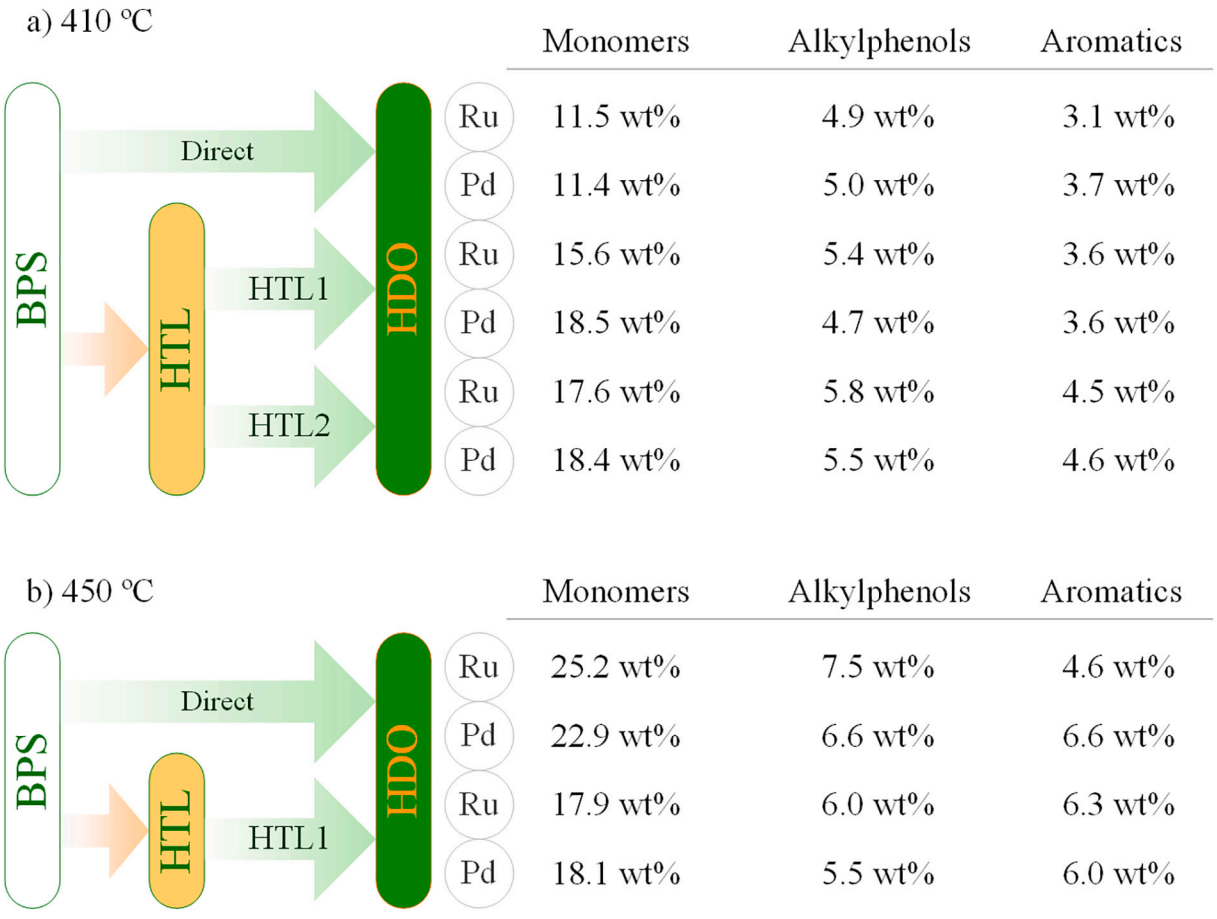

Fig. 10. Overview of total monomer, alkylphenols, and aromatic yields obtained from the hydrotreated oils on a starting BPS intake basis for the direct HDO and 2-step HTL-HDO approach at a) 410 °C and b) 450 °C using the Ru/C and Pt/C catalysts.

4. Conclusions

The direct HDO and HTL of a 2nd generation bioethanol production stillage (BPS) were compared, targeting the production of valuable monomers, specifically alkylphenols, and aromatics. Two commercial Ru/C and Pd/C catalysts were used in the HDO step, at different reaction conditions (375–450 °C). In comparison to HTL, HDO is a more suitable approach for the direct conversion of BPS, even though the energy efficiency is lower, as it leads to oils with higher volatility and higher amounts of low molecular weight alkylphenols/aromatics. For comparison, a 2-step HTL-HDO strategy was compared with the direct HDO approach. The results imply that an initial HTL step is an excellent pretreatment for the valorization of BPS using HDO without a dramatic decrease in the energy efficiency and may (i) solve feeding issues related to solid BPS feeding at high pressures in continuous reactors and (ii) preventing coke formation in the HDO stage, which is expected to improve process stability and catalyst lifetime. This two-step HTL-HDO approach does not have a major detrimental impact on the total alkylphenol+aromatic yields (13.2 wt% vs 12.3 wt% on an initial BPS intake basis through the direct HDO and HTL-HDO approach, respectively).

The findings reported in this study are of relevance to improve the economic viability of biomass conversions using HTL and HDO approaches and to boost innovations in the biobased economy. Future research on the use of continuous HDO reactors for the upgrading of the HTL oils and optimization of process conditions for maximizing yields of unsaturated monomer yields, and also including catalyst deactivation studies, will be required and is the subject of future studies in our groups.

Declaration of Competing Interest

The authors declare that they have no known competing financial interests or personal relationships that could have appeared to influence the work reported in this paper.

Acknowledgements

Dr. Idoia Hita is grateful for her postdoctoral grant awarded by the Department of Education, University and Research of the Basque Government (grant number POS_2015_1_0035). Leon Rohrbach, Jan Henk Marsman, Erwin Wilbers, Marcel de Vries, and Anne Appeldoorn are acknowledged for their technical and analytical support. Hans van der Velde is thanked for performing the elemental analysis.

Appendix A. Supplementary data

Supplementary data to this article can be found online at https://doi.org/10.1016/j.fuproc.2020.106654.

References

[1] P.S. Bezergianni, A. Dimitriadis, O. Kikhtyanin, D. Kubi Cka, Refinery co-processing of renewable feeds, Prog. Energy Combust. Sci. 68 (2018) 29–64.
[2] J. Moncada, V. Aristizábal, C.A. Cardona, Design strategies for sustainable biorefineries, Biochem. Eng. J. 116 (2016) 122–134.
[3] A.C. Neto, M.J.O.C. Guimarães, E. Freire, Business models for commercial scale second-generation bioethanol production, J. Clean. Prod. 184 (2018) 168–178.
[4] H.B. Aditiya, T.M.I. Mahlia, W.T. Chong, H. Nur, A.H. Sebayang, Second generation bioethanol production: a critical review, Renew. Sust. Energ. Rev. 66 (2016) 631–653.
[5] J.I. Santos, U. Fillat, R. Martin-Sampedro, I. Ballesteros, P. Manzanares, M. Ballesteros, M.E. Eugenio, D. Ibarra, Lignin-enriched fermentation residues from bioethanol production of fast-growing poplar and forage sorghum, BioResources. 10 (2015) 5203–5214.
[6] N.R. Baral, A. Shah, Techno-economic analysis of utilization of stillage from a cellulosic biorefinery, Fuel Process. Technol. 166 (2017) 59–68.
[7] W. Schutyser, T. Renders, S. Van Den Bosch, S.F. Koelewijn, G.T. Beckham, B. F. Sels, Chemicals from lignin: an interplay of lignocellulose fractionation, depolymerisation, and upgrading, Chem. Soc. Rev. 47 (2018) 852–908.
[8] S. Kang, X. Li, J. Fan, J. Chang, Hydrothermal conversion of lignin: a review, Renew. Sust. Energ. Rev. 27 (2013) 546–558.
[9] H.A. Baloch, S. Nizamuddin, M.T.H. Siddiqui, S. Riaz, A.S. Jatoi, D.K. Dumbre, N. M. Mubarak, M.P. Srinivasan, G.J. Griffin, Recent advances in production and upgrading of bio-oil from biomass: a critical overview, J. Environ. Chem. Eng. 6 (2018) 5101–5118.
[10] X.-F. Zhou, Conversion of Kraft lignin under hydrothermal conditions, Bioresour. Technol. 170 (2014) 583–586.
[11] K.R. Arturi, M. Strandgaard, R.P. Nielsen, E.G. Søgaard, M. Maschietti, Hydrothermal liquefaction of lignin in near-critical water in a new batch reactor: Influence of phenol and temperature, J. Supercrit. Fluids 123 (2017) 28–39.
[12] R. Singh, A. Prakash, S. Kumar Dhiman, B. Balagurumurthy, A.K. Arora, S.K. Puri, T. Bhaskar, Hydrothermal conversion of lignin to substituted phenols and aromatic ethers, Bioresour. Technol. 165 (2014) 319–322.
[13] L. Cao, I.K.M. Yu, Y. Liu, X. Ruan, D.C.W. Tsang, A.J. Hunt, Y.S. Ok, H. Song, S. Zhang, Lignin valorization for the production of renewable chemicals: State-of-the-art review and future prospects, Bioresour. Technol. 269 (2018) 465–475.
[14] J. Barbier, N. Ge Charon, N. Dupassieux, A. Loppinet-Serani, L. Mahé, J. Ponthus, M. Courtiade, A. Ducrozet, A.-A. Quoineaud, F. Cansell, Hydrothermal conversion of lignin compounds. A detailed study of fragmentation and condensation reaction pathways, Biomass Bioenergy 46 (2012) 479–491.
[15] M. Kleinert, T. Barth, Phenols from lignin, Chem. Eng. Technol. 31 (2008) 736–745.
[16] M. Oregui Bengoechea, N. Miletíc, M.H. Vogt, P.L. Arias, T. Barth, Analysis of the effect of temperature and reaction time on yields, compositions and oil quality in catalytic and non-catalytic lignin solvolysis in a formic acid/water media using experimental design, Bioresour. Technol. 234 (2017) 86–98.
[17] C. Løhre, G.-A.A. Laugerud, W.J.J. Huijgen, T. Barth, Lignin-to-Liquid-Solvolysis (LtL) of Organosolv Extracted Lignin, ACS Sustain. Chem. Eng. 6 (2018) 3102–3112.
[18] C. Liu, X. Wang, F. Lin, H. Zhang, R. Xiao, Structural elucidation of industrial bioethanol residual lignin from corn stalk: a potential source of vinyl phenolics, Fuel Process. Technol. 169 (2018) 50–57.
[19] B. Gómez-Monedero, M. Pilar Ruiz, F. Bimbela, J. Faria, Selective depolymerization of industrial lignin-containing stillage obtained from cellulosic bioethanol processing, Fuel Process. Technol. 173 (2018) 165–172.
[20] N. Priharto, F. Ronsse, W. Prins, I. Hita, P.J. Deuss, H.J. Heeres, Hydrotreatment of pyrolysis liquids derived from second-generation bioethanol production residues over NiMo and CoMo catalysts, Biomass Bioenergy 126 (2019) 84–93.
[21] D.S. Bajwa, X. Wang, E. Sitz, T. Loll, S. Bhattacharjee, Application of bioethanol derived lignin for improving physico-mechanical properties of thermoset biocomposites, Int. J. Biol. Macromol. 89 (2016) 265–272.
[22] S.J. Lee, H.J. Kim, E.J. Cho, Y. Song, H.-J. Bae, Isolation and characterization of lignin from the oak wood bioethanol production residue for adhesives, Int. J. Biol. Macromol. 72 (2015) 1056–1062.
[23] L. Fan, Y. Zhang, S. Liu, N. Zhou, P. Chen, Y. Cheng, M. Addy, Q. Lu, M. Mubashar Omar, Y. Liu, Y. Wang, L. Dai, E. Anderson, P. Peng, H. Lei, R. Ruan, Bio-oil from fast pyrolysis of lignin: Effects of process and upgrading parameters, Bioresour. Technol. 241 (2017) 1118–1126.
[24] P.J. de Wild, W.J.J. Huijgen, A. Kloekhorst, R.K. Chowdari, H.J. Heeres, Biobased alkylphenols from lignins via a two-step pyrolysis – Hydrodeoxygenation approach, Bioresour. Technol. 229 (2017) 160–168.
[25] I. Hita, T. Cordero-Lanzac, F.J. García-Mateos, M.J. Azkoiti, J. Rodríguez-Mirasol, T. Cordero, J. Bilbao, Enhanced production of phenolics and aromatics from raw bio-oil using HZSM-5 zeolite additives for PtPd/C and NiW/C catalysts, Appl. Catal. B Environ. 259 (2019) 118112.
[26] T. Cordero-Lanzac, I. Hita, F.J. García-Mateos, P. Castaño, J. Rodríguez-Mirasol, T. Cordero, J. Bilbao, Adaptable kinetic model for the transient and pseudo-steady states in the hydrodeoxygenation of raw bio-oil, Chem. Eng. J. 400 (2020) 124679.
[27] C.R. Kumar, N. Anand, A. Kloekhorst, C. Cannilla, G. Bonura, F. Frusteri, K. Barta, H.J. Heeres, Solvent free depolymerization of Kraft lignin to alkyl-phenolics using supported NiMo and CoMo catalysts, Green Chem. 17 (2015) 4921–4930.
[28] I. Hita, H.J. Heeres, P.J. Deuss, Insight into structure–reactivity relationships for the iron-catalyzed hydrotreatment of technical lignins, Bioresour. Technol. 267 (2018) 93–101.
[29] I. Hita, P.J. Deuss, G. Bonura, F. Frusteri, H.J. Heeres, Biobased chemicals from the catalytic depolymerization of Kraft lignin using supported noble metal-based catalysts, Fuel Process. Technol. 179 (2018) 143–153.
[30] S. Agarwal, R.K. Chowdari, I. Hita, H.J. Heeres, Experimental Studies on the Hydrotreatment of Kraft Lignin to Aromatics and Alkylphenolics using Economically Viable Fe-based Catalysts, ACS Sustain. Chem. Eng. 5 (2017) 2668–2678.
[31] S. Domalski, T.L. Jobe, T.A. Milne, Thermodynamic Data for Biomass Conversion and Waste Incineration, 2013.
[32] R.A. Sheldon, Green chemistry, catalysis and valorization of waste biomass, J. Mol. Catal. A: Chem. 422 (2016) 3–12.
[33] S. Ghysels, F. Ronsse, D. Dickinson, W. Prins, Production and characterization of slow pyrolysis biochar from lignin-rich digested stillage from lignocellulosic ethanol production, Biomass Bioenergy 122 (2019) 349–360.
[34] F. Mariotti, D. Tomé, P.P. Mirand, Converting nitrogen into protein—beyond 6.25 and Jones' factors, Crit. Rev. Food Sci. Nutr. 48 (2008) 177–184.
[35] B. Pang, S. Yang, W. Fang, T.-Q. Yuan, D.S. Argyropoulos, R.-C. Sun, Structure-property relationships for technical lignins for the production of lignin-phenol-formaldehyde resins, Ind. Crop. Prod. 108 (2017) 316–326.
[36] L. Lagerquist, A. Pranovich, I. Sumerskii, S. Von Schoultz, L. Vähäsalo, S. Willför, P. Eklund, Structural and thermal analysis of softwood lignins from a pressurized

hot water extraction biorefinery process and modified derivatives, Molecules. 24 (2019) 335–350.
[37] M.B. Figueirêdo, P.J. Deuss, R.H. Venderbosch, H.J. Heeres, Catalytic hydrotreatment of pyrolytic lignins from different sources to biobased chemicals: Identification of feed-product relations, Biomass Bioenergy 134 (2020) 105484.
[38] M.B. Figueirêdo, P.J. Deuss, R.H. Venderbosch, H.J. Heeres, Valorization of Pyrolysis Liquids: Ozonation of the Pyrolytic Lignin Fraction and Model Components, ACS Sustain. Chem. Eng. 7 (2019) 4755–4765.
[39] F. Sher, S.Z. Iqbal, H. Liu, M. Imran, C.E. Snape, Thermal and kinetic analysis of diverse biomass fuels under different reaction environment: a way forward to renewable energy sources, Energy Convers. Manag. 203 (2020) 112266.
[40] J.F. Saldarriaga, R. Aguado, A. Pablos, M. Amutio, M. Olazar, J. Bilbao, Fast characterization of biomass fuels by thermogravimetric analysis (TGA), Fuel. 140 (2015) 744–751.
[41] M. Nishida, T. Tanaka, T. Miki, T. Ito, K. Kanayama, Multi-scale instrumental analyses for structural changes in steam-treated bamboo using a combination of several solid-state NMR methods, Ind. Crop. Prod. 103 (2017) 89–98.
[42] P. Sannigrahi, D.H. Kim, S. Jung, A. Ragauskas, Pseudo-lignin and pretreatment chemistry, Energy Environ. Sci. 4 (2011) 1306–1310.
[43] A. Kloekhorst, H.J. Heeres, Catalytic Hydrotreatment of Alcell Lignin using Supported Ru, Pd, and Cu Catalysts, ACS Sustain. Chem. Eng. 3 (2015) 1905–1914.
[44] I. Hita, A. Gutiérrez, M. Olazar, J. Bilbao, J.M. Arandes, P. Castaño, Upgrading model compounds and scrap Tires Pyrolysis Oil (STPO) on hydrotreating NiMo catalysts with tailored supports, Fuel. 145 (2015) 158–169.
[45] S. Cheng, L. Wei, J. Julson, M. Rabnawaz, Upgrading pyrolysis bio-oil through hydrodeoxygenation (HDO) using non-sulfided Fe-Co/SiO_2 catalyst, Energy Convers. Manag. 150 (2017) 331–342.
[46] B. Duan, Q. Wang, Y. Zhao, N. Li, S. Zhang, Y. Du, Effect of catalysts on liquefaction of alkali lignin for production of aromatic phenolic monomer, Biomass Bioenergy 131 (2019) 105413.
[47] M. Rana, G. Taki, M.N. Islam, A. Agarwal, Y.-T. Jo, J.-H. Park, Effects of Temperature and Salt Catalysts on Depolymerization of Kraft Lignin to Aromatic Phenolic Compounds, Energy Fuel 33 (2019) 6390–6404.
[48] M. Auersvald, B. Shumeiko, D. Vrtiška, P. Straka, M. Staš, P. Šimáček, J. Blažek, D. Kubička, Hydrotreatment of straw bio-oil from ablative fast pyrolysis to produce suitable refinery intermediates, Fuel. 238 (2018) 98–110.
[49] M. Tymchyshyn, C. Xu, Liquefaction of bio-mass in hot-compressed water for the production of phenolic compounds, Bioresour. Technol. 101 (2010) 2483–2490.
[50] R.M. Happs, K. Iisa, J.R. Ferrell, Quantitative 13C NMR characterization of fast pyrolysis oils, RSC Adv. 6 (2016) 102665–102670.
[51] H. Ben, A.J. Ragauskas, Heteronuclear single-quantum correlation-nuclear magnetic resonance (HSQC-NMR) fingerprint analysis of pyrolysis oils, Energy Fuel 25 (2011) 5791–5801.
[52] R.K. Chowdari, S. Agarwal, H.J. Heeres, Hydrotreatment of Kraft Lignin to alkylphenolics and aromatics using Ni, Mo, and W phosphides supported on activated carbon, ACS Sustain. Chem. Eng. 7 (2019) 2044–2055.
[53] A.R. Ardiyanti, A. Gutierrez, M.L. Honkela, A.O.I. Krause, H.J. Heeres, Hydrotreatment of wood-based pyrolysis oil using zirconia-supported mono- and bimetallic (Pt, Pd, Rh) catalysts, Appl. Catal. A Gen. 407 (2011) 56–66.
[54] R. Shakya, S. Adhikari, R. Mahadevan, E.B. Hassan, T.A. Dempster, Catalytic upgrading of bio-oil produced from hydrothermal liquefaction of Nannochloropsis sp, Bioresour. Technol. 252 (2018) 28–36.